ADVANCED MATERIALS

DOI: 10.1002/adma.200600673

Tuning Nanomaterials' Characteristics by a Miniaturized In-Line Dispersion–Precipitation Method: Application to Hydrotalcite Synthesis**

By *Sònia Abelló* and *Javier Pérez-Ramírez**

Coprecipitation is one of most frequently applied methods of preparing precursors of catalysts and support materials with good dispersion of the components, both in the laboratory and on an industrial scale.[1,2] This method is generally practiced in batch mode and involves feeding a solution containing the cations and a solution containing the precipitating agent (typically hydroxides and/or (bi)carbonates) into a mechanically stirred vessel at constant or variable pH. Time, temperature, stirring speed, pH, and order in which the cationic and anionic solutions are brought into contact are critical parameters that impact on the characteristics of the final material.[3] A well-known drawback associated with coprecipitation is related to the presence of pH gradients due to ineffective stirring of the reactor volume. Most importantly, owing to the discontinuous operation, the residence time of the precipitate particles and concentration of reactants change throughout the precipitation process, and the degree of nucleation and, mainly, crystal growth markedly vary between the start and end products.[4] This prevents a constant product quality being maintained throughout the whole precipitation process, which is often essential for the subsequent application of the resulting materials. The development of approaches exerting control on the precipitate characteristics would make headway towards achieving better defined and more efficient materials for fundamental studies and applications, respectively. Herein, we introduce a novel in-line dispersion–precipitation (ILDP) method for the preparation of nanomaterials with tunable properties. This was accomplished by performing the precipitation in continuous mode using a vigorously stirred microreactor with in-line pH control at fixed residence time. Simplicity, reproducibility, versatility, and scalability are key features of this highly intensified method. The potential of the ILDP is illustrated here for the synthesis of hydrotalcites.

[*] Prof. J. Pérez-Ramírez, Dr. S. Abelló
Laboratory for Heterogeneous Catalysis
Institute of Chemical Research of Catalonia (ICIQ)
Av. Països Catalans 16, Tarragona 43007 (Spain)
E-mail: jperez@iciq.es
Prof. J. Pérez-Ramírez
Catalan Institution for Research and Advanced studies (ICREA)
Pg. Lluís Companys 23, Barcelona 08010 (Spain)

[**] This research was financially supported by the ICIQ Foundation. M. Santiago is acknowledged for assistance in setting up the experimental apparatus. The research in this paper is described in European patent application EP06115 928.1. Supporting Information is available online from Wiley InterScience or from the author.

The principle of the ILDP method is schematically shown in Figure 1. The acid and base solutions are fed by means of peristaltic pumps into a home-made microreactor with an effective volume of ca. 6 mL. The precipitation chamber incorporates a rotating element attached to a high-speed disperser (up to 24 000 rpm) and static blades in the periphery of the main axis. This enables an impressively high degree of mixing, leading to impeller Reynolds (Re) numbers[5] up to 10^5 (turbulent regime at $Re > 10^4$). An in-line probe measures the pH of the slurry directly at the outlet of the microreactor and is connected to one of the pumps to maintain a constant pH. The possibility of varying the residence time by changing the flow of feed solutions enables faster or slower precipitations to be conducted, impacting on complex interconnected nucleation–crystal growth–agglomeration processes, and thus on the characteristics of the final product (see below). This configuration is perfectly in tune with the trend of intensifying unit operations in industry, as miniaturization of the precipitation chamber leads to markedly increased productivities compared to conventional batch precipitation.

Hydrotalcites have been widely applied as adsorbents, anion exchangers, flame retardants, and catalysts and catalyst supports in environmental as well as fine and bulk chemistry applications.[6,7] They are often synthesized by batch coprecipitation and several parameters have been varied in the preparation in order to alter the physicochemical characteristics of the final product, such as conducting the precipitation at different pH,[3] levels of supersaturation,[6] and temperature[8] or by means of sol–gel synthesis.[9] Postsynthesis modifications such as aging and hydrothermal treatments have also been performed,[8,10,11] in conjunction with application of microwaves[12,13] or ultrasound.[14] However, despite much effort, a solid understanding of the nucleation and crystal-growth phenomena associated with the precipitation and post-treatments in order to tune hydrotalcite characteristics is not yet achieved. Very recently, Evans and Duan[15] proposed a discontinuous method using a colloid mill to prepare hydrotalcites with a narrow size range of large crystallites (60–80 nm).

Table 1 shows characterization results of Mg–Al hydrotalcite samples prepared by the ILDP method at different stirring speeds (ω) and residence times (τ), and the reference sample prepared by standard batch coprecipitation.[6] In all cases, the minute concentration of Mg^{2+} and Al^{3+} determined in the filtrates revealed that the degree of precipitation at the tested conditions was almost complete (>99%). In line with

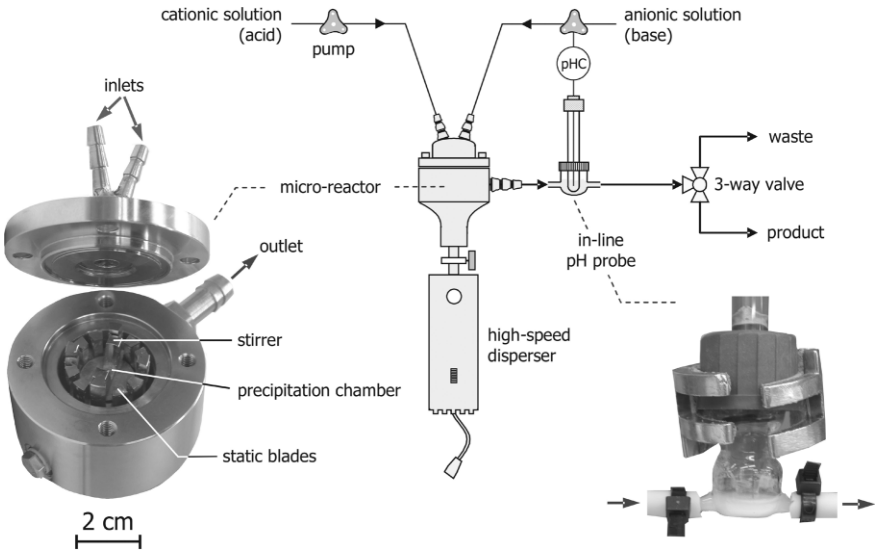

Figure 1. ILDP setup, with photographs of the precipitation microreactor and the in-line pH probe.

Table 1. Properties of the differently synthesized hydrotalcites.

	τ [a] [s]	ω [b] [rpm]	Mg/Al molar ratio	$\bar{D}$ [c] [nm]	S_{BET} [d] [$m^2 g^{-1}$]	V_{pore} [e] [$cm^3 g^{-1}$]
HT-1	36	13 500	2.8	6.4	69	0.29
HT-2	36	24 000	2.7	11.0	85	0.45
HT-3	12	24 000	2.8	5.2	130	0.78
HT-4	4.5	13 500	2.6	5.8	9	0.01
HT-5	4.5	24 000	2.7	5.3	111	0.32
HT-6	1	24 000	2.7	3.9	0.6	0.0
HT-batch	3600 [f]	500	2.8	38	50	0.38

[a] Residence time. [b] Stirring speed. [c] Average crystallite size from the Scherrer equation applied to the 003 reflection. [d] Specific surface area by the Brunauer–Emmett–Teller (BET) method [16]. [e] Pore volume. [f] Duration of the addition of acid and base solutions to the precipitation vessel.

this, chemical analysis showed that the Mg/Al molar ratio in the solids was in the narrow range of 2.6–2.8, very close to the nominal value of 3.

A visual inspection of the samples (Fig. 2) already reveals the striking impact on the resulting products of applying extreme residence times. The solid obtained by *flash* precipitation ($\tau = 1$ s) is translucent and shiny, in contrast to the typical opaque appearance of the sample precipitated at longer residence times or discontinuously. The mechanical properties of the solid precipitated at shorter or longer residence times also differ dramatically. The particles at $\tau = 36$ s can be easily fractured as compared to the much harder product obtained by coprecipitation at $\tau = 1$ s. The surface of the particles in the latter sample was very smooth and extremely difficult to scratch.

As shown in the Supporting Information, all samples exhibit hydrotalcite as the only crystalline phase. Upon decreasing the residence time in the precipitation microreactor, broader and less-intense X-ray diffraction (XRD) reflections appear, as smaller crystallites are obtained. The average crystallite size $\bar{D}$ of the samples was estimated from the Scherrer equation[17] using the basal 003 reflection, that is, in the *c*-direction. Very small crystallites of ca. 4 nm were obtained in HT-6 ($\tau = 1$ s), and their size hardly changed upon increasing the residence time up to $\tau = 18$ s, but tripled in HT-2 ($\tau = 36$ s) (Fig. 3a). The complete precipitation at residence times of $\tau = 1$ s confirmed that the nucleation process is extremely fast. The increase in average crystallite size on increasing the residence time from 18 s (5 nm) to 36 s (12 nm) strongly suggests that crystal growth and particle agglomeration processes become prominent on that time scale. These can be effectively minimized by carrying out preparations at $\tau < 18$ s. As expected, the largest crystallites (ca. 40 nm) were obtained in the reference Mg–Al hydrotalcite prepared by batch coprecipitation. The latter preparation lasted 1 h and crystal growth and agglomeration processes take place to a larger extent, leading to broad particle size distributions. Whenever visible in the XRD pattern, the average crystallite size was also determined from the nonbasal 110 reflection (*a*-direction). Similarly to what was obtained from the 003 determination, larger crystallites were estimated with increasing residence time, and particularly in the batch-precipitated sample. Expectedly, values of $\bar{D}$ from the 110 reflection are somewhat larger than from the 003 reflection, as a consequence of the platelet-shaped crystallites.

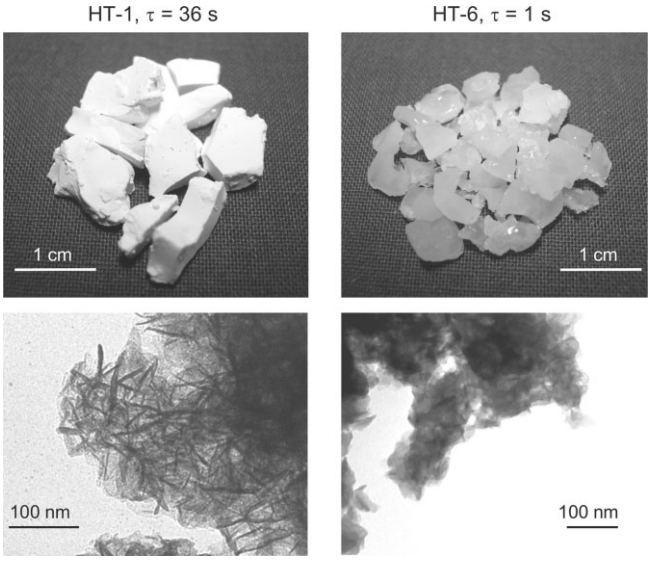

Figure 2. Photographs of the Mg–Al hydrotalcites resulting from the ILDP method at extreme residence times, and corresponding transmission electron microscopy images.

ADVANCED MATERIALS

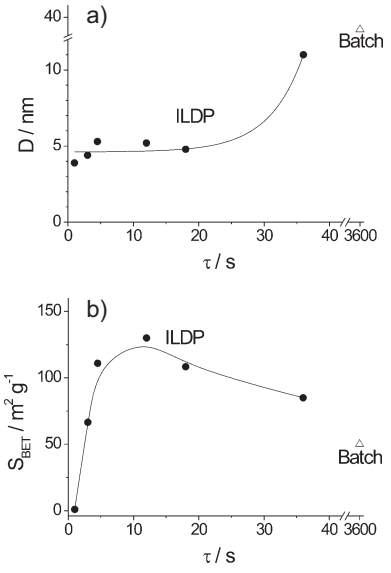

Figure 3. Average crystallite size (a) and surface area (b) of the hydrotalcite samples versus the residence time in the ILDP microreactor at $\omega = 24\,000$ rpm. Open triangles: batch-precipitated sample.

The effect of the stirring speed on the crystallite size largely depends on the residence time. At $\tau = 4.5$ s, the average crystallite size was practically the same upon stirring at 13 500 or 24 000 rpm (samples HT-4 and HT-5). However, when the residence time was increased to $\tau = 36$ s, the average crystallite size increased upon increasing the stirring speed (compare samples HT-1 and HT-2). The latter result can be tentatively explained by the local heating of the microreactor volume at very high rotation speeds, which accelerates both crystallite growth and crystal agglomeration into larger particles. The extent of growth and agglomeration processes is obviously reduced at shorter residence times, and the effect of heating due to higher rotation speeds on the crystallite size was unnoticeable. It has to be emphasized that most of the sample preparations reported in this Communication were repeated several times. We found excellent reproducibility of the ILDP method based on the obtained characterization results.

The achievement of small crystallites in coprecipitation is typically accomplished by increasing the degree of supersaturation.[2] A high degree of supersaturation leads to a large number of small nuclei of uniform size, and the opposite applies at low or medium degree of supersaturation.[4] The syntheses reported here were conducted at fixed supersaturation conditions. Consequently, the small crystallites at $\tau < 18$ s in Figure 3 are basically related to the minimization of agglomeration phenomena. The time scale for nucleation is much faster than that of crystal growth,[2] so the residence time makes it possible to decouple these processes or combine them in order to produce materials with different characteristics.

In order to gain insights into the morphology of the differently synthesized hydrotalcites, transmission electron microscopy (TEM) analyses were conducted (Fig. 2). HT-1 ($\tau = 36$ s and $\omega = 13\,500$ rpm) exhibited randomly distributed aggregates of fibrous particles with lengths up to 80 nm, characteristic of hydrotalcites prepared by conventional batch coprecipitation.[18] Each filament consists of a large number of platelets. Particles in HT-1 tend to aggregate in an edge–face manner, as reported by Yun and Pinnavaia.[3] As shown in Table 1, an increase of stirring speed from 13 500 to 24 000 rpm at $\tau = 36$ s led to larger agglomerates of crystals (see TEM image of HT-2 in Supporting Information). Conversely, HT-6 ($\tau = 1$ s) exhibits a completely different morphology, characterized by particles with poorly defined shape and a marked degree of face-to-face agglomeration. This was unexpected in view of the very similar crystallite size at $\tau \leq 12$ s determined by XRD.

The porous properties of the hydrotalcites synthesized at different residence times were assessed by N_2 physisorption. The adsorption–desorption isotherms of the hydrotalcites can be classified as type IIb (see example in Supporting Information), which is characteristic of slit-shaped pores between aggregates of platelet particles.[19] As shown in Figure 3b, the BET surface area of the samples versus the residence time goes through a maximum. The porous properties of the samples in the optimum τ range of 4.5–18 s (S_{BET} and V_{pore} up to 130 $m^2 g^{-1}$ and 0.78 $cm^3 g^{-1}$, respectively) are superior to those of the samples using $\tau = 36$ s and that prepared by batch precipitation ($S_{BET} = 50$ $m^2 g^{-1}$ and $V_{pore} = 0.39$ $cm^3 g^{-1}$). This is likely a consequence of the smaller crystallites in the former samples. The hydrotalcite prepared at $\tau = 1$ s consists of 4 nm crystallites (Fig. 3a), but both surface area and pore volume are close to zero. Accordingly, the ILDP method working at ultrashort residence times (*flash* coprecipitation) makes it possible to obtain synthetic clays with small crystallites that are extremely well packed into large crystal assemblies with smooth surfaces. This explains the low S_{BET} of the latter sample, since a spherical crystal of hydrotalcite of 1 μm would lead to an external surface area of 3 $m^2 g^{-1}$ (0.6 $m^2 g^{-1}$ was measured in HT-6, see Table 1). This unprecedented property, which cannot be explained in detail at the present stage, expands the already broad applications of hydrotalcite-like compounds, for example in ceramic films and nanolithographic processing.

In summary, we have demonstrated the potential of the in-line dispersion–precipitation (ILDP) method for preparing nanomaterials with tunable properties. Continuous operation in a miniaturized microreactor, adjustable residence time, and excellent mixing are key benefits of this highly intensified, reproducible, and versatile method. In fact, the small volume of the precipitation chamber (6 mL) and the ability to work with short residence times (<10 s) enables productivities of several tons of product per hour and cubic meter of reactor to be achieved, up to three orders of magnitude higher than those obtained by typical discontinuous (co)precipitation in large reactor vessels. The applicability of the ILPD method to the synthesis of other types of materials with predictable properties should be highlighted. Apart from the case study of Mg–Al hydrotalcites illustrated in this Communication, we have

successfully applied the ILDP method to the synthesis of different hydrotalcite compositions (varying the combination of metals and their molar ratio) and other clay-type materials such as metal-substituted dawsonites[20]. Hence, we expect it to become a widely used approach to overcoming well-known drawbacks of the often applied batch precipitation.

Experimental

Mg–Al hydrotalcites with a nominal Mg/Al molar ratio of three were prepared by the ILDP method (see Fig. 1). Aqueous solutions of $Mg(NO_3)_2{\cdot}6H_2O$ (0.75 M) and $Al(NO_3)_3{\cdot}9H_2O$ (0.25 M) and the precipitating agent (NaOH + Na_2CO_3, each 1 M) were continuously fed at room temperature into the precipitation chamber keeping the pH constant at 10. The precipitation chamber was stirred at speeds in the range of 6 500–24 000 rpm. Residence time in the microreactor was varied in the range of 1–36 s. Filtration of the resulting slurry was carried out after the in-line pH probe upon reaching stable pH. The resulting solid was thoroughly washed and dried at 353 K. For comparative purposes, a reference Mg–Al hydrotalcite was prepared by conventional batch coprecipitation at pH 10 [6]. The chemical compositions of the solids and corresponding filtrates were determined by atomic absorption spectroscopy (AAS; Hitachi Z-8200) and inductively coupled plasma optical emission spectroscopy (ICP-OES; Perkin-Elmer Plasma 400). Powder XRD patterns were acquired in transmission on a D8 Bruker-Nonius Advance Series $2\theta/2\theta$ powder diffraction system using Cu Kα radiation. Data were collected in the 2θ range of 5° to 70° with an angular step of 0.016° and a counting time of 10.4 s per step. TEM was carried out with a Zeiss 10 CA microscope. The samples were mounted onto a carbon-coated copper grid by placing a few droplets of a suspension of the powder sample in chloroform on it, followed by evaporation at ambient conditions. N_2 adsorption and desorption isotherms at 77 K were measured on a Quantachrome Autosorb 1-MP after evacuation of the samples at 393 K for 16 h.

Received: March 29, 2006
Final version: May 2, 2006

[1] R. A. van Santen, P. W. N. M. van Leeuwen, J. A. Moulijn, B. A. Averill, *Catalysis: An Integrated Approach*, 2nd ed., Elsevier Science, Oxford **1999**.
[2] F. Schütz, K. Unger, in *Handbook of Heterogeneous Catalysis*, Vol. 2 (Eds: G. Ertl, H. Knözinger, J. Weitkamp), Wiley-VCH, Weinheim **1997**, pp. 72–86.
[3] S. K. Yun, T. J. Pinnavaia, *Chem. Mater.* **1995**, *7*, 348.
[4] P. Courty, C. Marcilly, in *Preparation of Catalysts III*, Studies in Surface Science and Catalysis, Vol. 16 (Eds: G. Poncelet, P. Grange, P. A. Jacobs), Elsevier Science, Amsterdam **1983**, pp. 485–517.
[5] *Perry's Chemical Engineers' Handbook*, 7th ed. (Eds: R. H. Perry, D. W. Green, J. O. Maloney), McGraw-Hill, New York **1997**.
[6] F. Cavani, F. Trifirò, A. Vaccari, *Catal. Today* **1991**, *11*, 173.
[7] P. S. Braterman, Z. P. Xu, F. Yarberry, in *Handbook of Layered Materials* (Eds: S. M. Auerbach, K. A. Carrado, P. K. Dutta), Taylor & Francis, New York **2004**, pp. 313–372.
[8] F. Kovanda, D. Kolousek, Z. Cílová, V. Hulínský, *Appl. Clay Sci.* **2005**, *28*, 101.
[9] F. Prinetto, G. Ghiotti, P. Graffin, D. Tichit, *Microporous Mesoporous Mater.* **2000**, *39*, 229.
[10] L. Hickey, J. T. Kloprogge, R. L. Frost, *J. Mater. Sci.* **2000**, *35*, 4347.
[11] J.-M. Oh, S.-H. Hwang, J.-H. Choy, *Solid State Ionics* **2002**, *151*, 285.
[12] S. Kannan, R. V. Jasra, *J. Mater. Chem.* **2000**, *10*, 2311.
[13] G. Fetter, F. Hernández, A. M. Maubert, V. H. Lara, P. Bosch, *J. Porous Mater.* **1997**, *4*, 27.
[14] M. J. Climent, A. Corma, S. Iborra, K. Epping, A. Velty, *J. Catal.* **2004**, *225*, 316.
[15] D. G. Evans, X. Duan, *Chem. Commun.* **2006**, 485.
[16] S. Brunauer, P. H. Emmett, E. Teller, *J. Am. Chem. Soc.* **1938**, *60*, 309.
[17] P. Scherrer, *Göttingen Nachr.* **1918**, *2*, 98.
[18] W. T. Reichle, S. Y. Kang, D. S. Everhardt, *J. Catal.* **1986**, *101*, 352.
[19] F. Rouquerol, J. Rouquerol, K. Sing, *Adsorption by Powders and Porous Solids*, Academic, London **1999**.
[20] M. Santiago, M. S. Yarfani, J. Pérez-Ramírez, *J. Mater. Chem.* **2006**, *16*, 2886.

